INFLATION PRESSURE AND STATIC LOAD EFFECTS ON CONTACT CHARACTERISTICS AT SOLID SOIL – TIRE INTERFACE

Nicoleta UNGUREANU[1], Gheorghe VOICU[2], Valentin VLĂDUȚ[3], Sorin-Ştefan BIRIŞ[4], Mihai MATACHE[5]

The paper presents the results of some experimental research on the influence of factors such as the external load and tire inflation pressure on the footprint area between a rigid surface and the tire of an agricultural trailer. These two factors determine, through the footprint area, the depth at which the equivalent stresses are distributed in the soil, and thus the intensity of artificial soil compaction. To limit soil compaction, the contact area should to be as large as possible, so that the contact pressure on the soil to be lower and the equivalent stresses do not propagate to large depths in the soil. At high tire inflation pressures the contact area is smaller, contact pressure will be higher, and the soil will be compacted at greater depths, with negative ecological and agronomic consequences. The tests were carried out on five static external loads (wheel loads) and for each load were used five values of tire inflation pressure.

Keywords: tire inflation pressure, external load, footprint area, contact pressure

1. Introduction and review

According to *Soil Science Society of America*, soil compaction represents "the process by which the soil grains are rearranged to decrease void space and bring them into closer contact with one another, thereby increasing the bulk density" [12, 13].

From an ecological perspective, soil compaction leads to: erosion, landslides, flooding, leakage of pesticides and nutrients in groundwater, increasing of the emanations of N_2O, CH_4 and CO_2, rut formation (being one of the first visible signs of soil degradation by the passage of agricultural vehicles) [2, 6, 8, 15, 22]. From an agronomical perspective, soil compaction leads to: increasing penetration resistance, inhibition of root development and plant growth, followed by low productivity of crops, increasing resistance to plowing and consequently higher fuel consumption [6, 9, 14, 15, 16, 17, 19].

[1] Ph.D. Stud., Dep. of Biotechnical Systems, University POLITEHNICAof Bucharest, Romania, e-mail: nicoletaung@yahoo.com
[2] Prof., Dep. of Biotechnical Systems, University POLITEHNICA of Bucharest, Romania
[3] Ph.D. eng., National Research - Development Institute For Machines And Installations Designed To Agriculture And Food Industry, Romania
[4] Prof., Dep. of Biotechnical Systems, „Politehnica" University of Bucharest, Romania
[5] Ph.D. Stud., National Research - Development Institute For Machines And Installations Designed To Agriculture And Food Industry, Romania

According to literature, among the factors influencing artificial compaction of soil, the most important ones are: soil type (structure, texture) [1, 3, 4, 5, 10], moisture content [1, 3, 4, 5, 10], bulk density [10], mass of agricultural machinery [5], size of external load [1, 3, 4, 10], shape of footprint [3, 4], footprint (contact) area [3, 4], tire inflation pressure [1], contact pressure [5, 10], number of passes on soil [1, 3, 4, 5, 10], speed of the agricultural vehicle [1, 5, 10], vibrations [10].

After [16], the process of artificial compaction has four stages (see Fig. 1): tire of agricultural machinery applies stresses on soil surface; the size of external load determines the size of stress applied on the soil; the higher the external load, the larger the depth at which stress is distributed in the soil; as a reaction to the applied stress, soil deforms (the deformation depends on soil mechanical resistance); soil deformation leads to changes in soil structure and porosity. Between these four stages, there are a series of links. The stress-strain behavior of soil influences the stress at soil surface and the distribution of stress in the soil depth, and the change of soil porosity influences its water retention capacity and soil resistance.

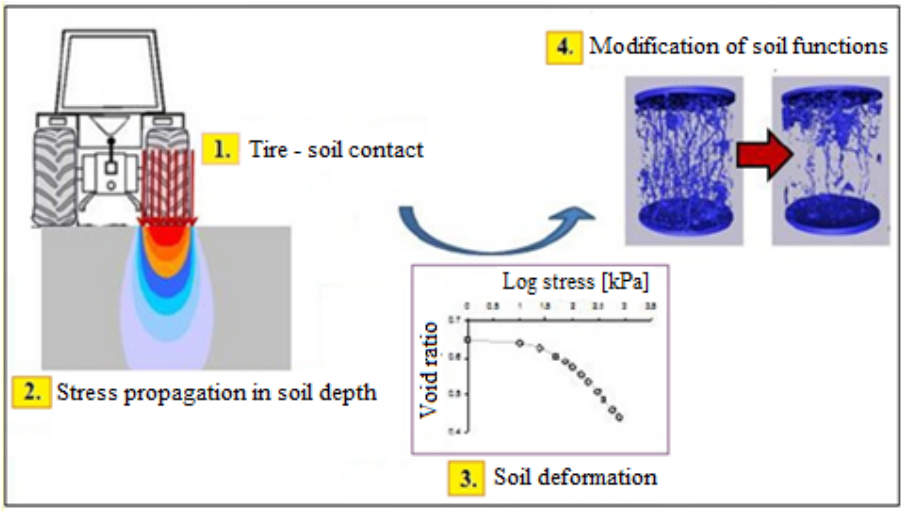

Fig. 1. Stages of compaction, from soil stress to soil deformation and changes in soil structure and porosity, [16]

The term “contact area” refers to the portion of wheel or tire in contact with the supporting surface, which is an important factor for the load capacity of the tire. “Static contact area” is the contact area between tire and a rigid or deformable surface, when the tire is loaded statically, without having forwarding movement [23]. For agricultural soils, due to higher tire pressures, smaller footprint areas are formed, soil deformation is larger and stress is distributed

deeper into the soil. At lower tire inflation pressures, tire deforms more, footprint area increases, mean pressures in the footprint are lower, soil deformation is lower and stresses are distributed to shallower depths [3].

2. Theoretical considerations

In contact with the soil, the tire leaves a footprint (i.e. contact patch) whose shape and size depends on several categories of factors: soil type and its physical characteristics, type of tire (stiffness, tread), tire inflation pressure, the force exerted on the wheel (i.e. external load or load wheel). In contact with a dry hard soil (e.g. road), a tire deforms both longitudinally and transversely, and the footprint size and shape will be given by tire inflation pressure and by external load. In this situation, the footprint mainly tends to have a rectangular shape with rounded corners (more or less) and less to have an elliptical shape.

Determining the shape and size (area) of the footprint is particularly important, both for auto vehicles and also for tractors and agricultural machinery. If for the auto vehicles the importance falls primarily on the adhesion to the road, for tractors and agricultural machinery the importance is given to both adhesion and the pressure on soil (contact pressure), so that shallow and deep compaction to be kept small. Compaction not only affects energy consumption for agricultural works, but also the development and growth of crops. Therefore, it is necessary to make tests to determine the footprint of each type of tire and the influence of its constructive and functional characteristics, in order to determine the most convenient pressures and stresses for the proper development of plants and to reduce energy consumption. At the contact with a hard soil can be established the shape of footprint and the geometrical dimensions of the footprint, and experimental tests should start with these, under the influence of external load and tire inflation pressure.

In paper [11] was studied the variation of the contact area and pressure distribution in the footprint between a GoodYear tire, model 13/7.5-16 SL (tire width 0.33 m) and soil in two cases: in the presence, respectively in the absence of a 0.3 m thick layer of sand between the tire and the soil. In both cases, wheel load was 1.5 tons and tire inflation pressure was 180 kPa. Without the layer of sand under the tire, the footprint was 0.29 m length and 0.3 m width, and maximum contact pressure of 561 kPa was recorded on footprint outline. In the presence of the sand layer under the tire, the footprint was 0.406 m length and 0.365 m width (values higher with 35 % and 23 % than those measured in the absence of the layer of sand) and the maximum contact pressure of 186 kPa was recorded along the centerline of the tire.

Paper [19] addresses the distribution of pressure in the footprint between a sandy soil and two types of agricultural tire (650/65R 30.5 and 800/50R 34). Wheel

load was constant (60 kN), for tire inflation pressures of 50, 100 and 240 kPa. By reducing tire inflation pressure from 240 kPa to 50 kPa, the footprint doubled its dimensions. For both tires, increasing tire inflation pressure resulted in an increase of contact pressure by approximately 90 kPa with respect to the value of tire inflation pressure.

Influence of tire inflation pressure and size of external load on the footprint area between a sandy loam soil and tire was studied in paper [20]. Tire inflation pressure was variable (60, 80, 100 and 200 kPa), and for each of these values the external load was varied (11.8; 17.9; 25 and 32 kN). By increasing the external load and reducing tire inflation pressure, the contact area increased from 1400-2000 cm^2 for an external load of 1200 kg to 2400-3200 cm^2 for an external load of 3200 kg. By doubling the external load, a increase of 30-40 % in the contact area was obtained, while by doubling tire inflation pressure the contact area decreased by 70-80 % from its initial value. The distribution of contact pressure was uniform, almost linear with tire inflation pressure, the slope of the curves increasing with the increase of the external load.

Footprint area can be computed using the COMPSOIL model [**7**]:

$$A = s_1 \cdot b \cdot d + s_2 \cdot Q + s_3 \cdot \frac{Q}{p_i} \tag{1}$$

where: A – footprint area [m^2]; Q – external load [kN]; b – tire width [m]; d – tire overall diameter [m]; p_i – tire inflation pressure [kPa]; s_1, s_2, s_3 – empirical parameters depending on soil stiffness.

3. Materials and methods

The experiment was conducted in laboratory conditions, in the Testing Department for Tractors and Equipment for Agriculture and Food Industry, at the National Research - Development Institute For Machines And Installations Designed To Agriculture And Food Industry, Bucharest.

The objective of the experiment was to study the influence of tire inflation pressure and size of external load on the footprint area between hard soil and tire. In our paper was tested the right side rear wheel of the RM-5 biaxial transport trailer, equipped with an agricultural tire, model Danubiana 11.5 / 80-13.5 profile D179 (tire width 290 mm, tire diameter 845 mm).

Tests were performed on concrete, and stresses at the interface with the terrain and the size of footprint were determined by interposing between the two elements an Tekscan Industrial Sensing sensor for measuring the contact pressure (with minimum size of sensitive surface 850 mm x 550 mm), connected to an electronic data acquisition system VersaTek Handle (see Figure 2). During the tests, the values of external load were varied (4.56 kN; 9.22 kN; 12.8 kN; 17.11

kN; 21.18 kN), and for each of these values the tire inflation pressure was also varied (180 kPa; 210 kPa; 240 kPa; 270 kPa; 300 kPa).

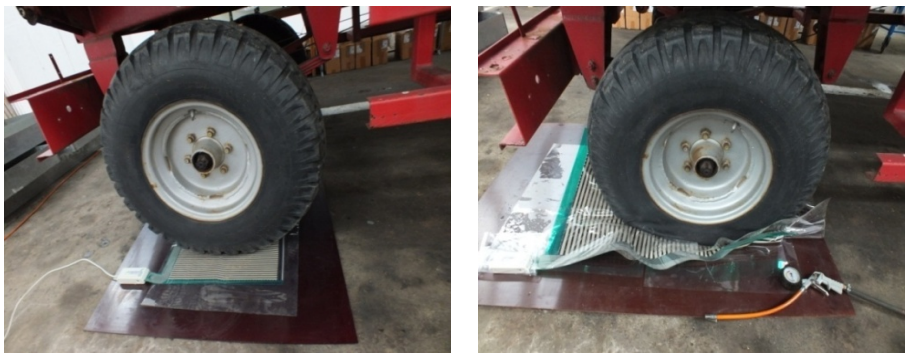

Fig. 2. Aspect during testing with maximum external load (21.18 kN), tire inflation pressure of 300 kPa (left), respectively tire deformation at tire inflation pressure of 180 kPa (right)

For each case, the geometrical dimensions of the obtained footprints and alsi the tire diameter were measured. Then, the contact pressure was calculated with the following equation:

$$p_c = \frac{Q}{A} \tag{2}$$

where: p_c– contact pressure [kPa]; Q – external load [kN]; A – footprint area [m^2].

4. Results and discussions

Experimental data, both for the values of input and output parameters considered and analyzed in this paper are presented in Table 1. The data obtained from the experiments were used to graphically plot the variation curves of footprint area between the soil and tire, depending on tire inflation pressure, external load and contact pressure on the soil.

From the analysis of the diagram in Figure 3 it can be observed that the footprint area approximately follows a linear distribution, proportional to the external load, regardless of the value of tire inflation pressure. Regression analysis, conducted in MSOffice Excel program, shows a high degree of correlation of the experimental data with the law of linear variation of over 0.965, in all five cases analyzed, which proves that the footprint area is directly proportional to the increase of external load. If for loads of approximately 5 kN, footprint area has values between 0.023 and 0.03 m^2, these values increase from 0.074 to 0.1 m^2 for a load of about 21 kN load and for tire inflation pressures of 180 to 300 kPa.

Table 1

Values of measured and determined parameters

External load Q [kN]	*Tire inflation pressure p_i [kPa]*	*Footprint area A [m^2]*	*Contact pressure p_c [kPa]*	*Footprint width b [m]*	*Tire diameter d [m]*
4.56	180	0.0312	146.093	0.206	0.8225
	210	0.0297	153.185	0.203	0.8282
	240	0.0280	162.660	0.190	0.8306
	270	0.0257	177.280	0.186	0.8315
	300	0.0234	194.788	0.156	0.8324
9.22	180	0.0497	185.479	0.242	0.7976
	210	0.0445	207.158	0.220	0.8097
	240	0.0416	221.544	0.208	0.8190
	270	0.0401	229.513	0.205	0.8229
	300	0.0369	249.236	0.203	0.8253
12.8	180	0.0658	194.254	0.252	0.7779
	210	0.0602	212.568	0.243	0.8017
	240	0.0562	227.628	0.237	0.8095
	270	0.0550	232.541	0.228	0.8121
	300	0.0509	251.133	0.220	0.8133
17.11	180	0.0867	197.343	0.288	0.7335
	210	0.0766	223.237	0.267	0.7466
	240	0.0728	234.930	0.239	0.7792
	270	0.0699	244.638	0.236	0.7877
	300	0.0664	257.402	0.220	0.8014
21.18	180	0.0988	214.283	0.248	0.7159
	210	0.0852	248.425	0.240	0.7380
	240	0.0777	272.436	0.238	0.7437
	270	0.0748	282.954	0.223	0.7883
	300	0.0734	288.524	0.220	0.7928

The same can be seen from the analysis of diagrams in Figure 4, which presents the variation of the footprint area depending on tire inflation pressure at various external loads. It can be noted that, by increasing the tire inflation pressure, the footprint area decreases proportionally, however this decrease being quite slow. Regression analysis performed on computer shows a decreasing linear distribution, and the correlation coefficient is relatively high (R^2 = 0.819 – 0.990). The footprint area values depending on the external load, at different tire inflation pressures, vary in a quite narrow range. However, the footprint area values depending on the tire inflation pressure, at different external loads, vary in a wider range (Figs. 3 and 4).

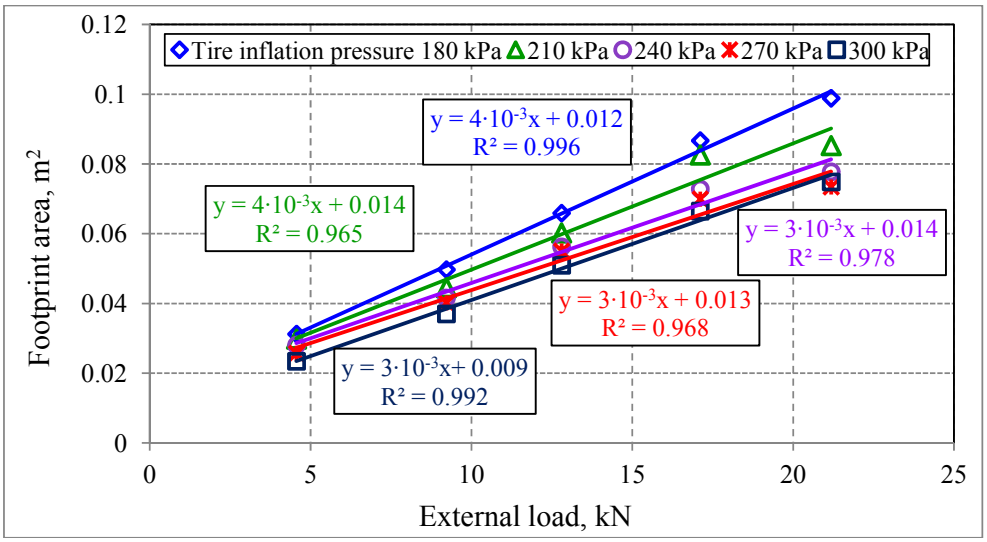

Fig. 3. Variation of footprint area with the external load, for various tire inflation pressures

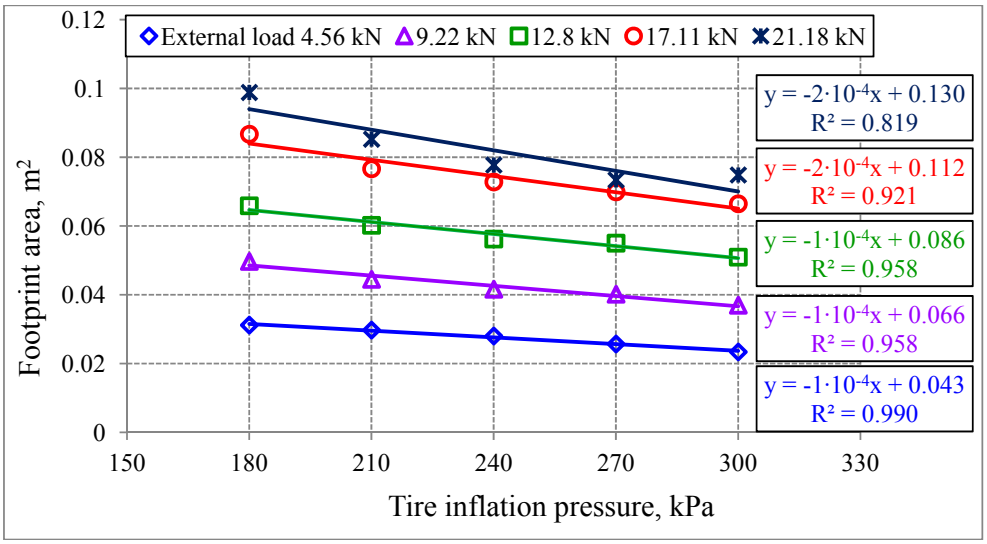

Fig. 4. Variation of footprint area with tire inflation pressure, for various values of external load

Thus, for tire inflation pressure of 180 kPa, the footprint area values range from about 0.03 m^2 for an external load of 4.56 kN, to approximately 0.1 m^2 for an external load of 21.18 kN. However, regression lines are not parallel to the variation of footprint area with the external load, as they open in fan shape for the

five values of tire inflation pressure, from the external load of 4.56 kN to 21.18 kN (the range of values increases from about 0.01 m^2 to approx. 0.025 m^2) and they follow the same trend at the variation of footprint area with tire inflation pressure. If the width of the range of values is about 0.07 m^2 at tire inflation pressure of 180 kPa (from the external load of 4.56 kN to 21.18 kN), it decreases to about 0.05 m^2 at tire inflation pressure of 300 kPa (for the same range of values of the external load).

Fi.g 5 shows the variation of footprint area depending on the contact pressure between soil and tire, for five values of the external load, along with the regression lines obtained in Excel program, which shows a very good correlation of experimental data with linear variation law ($R^2 \geq 0.991$).

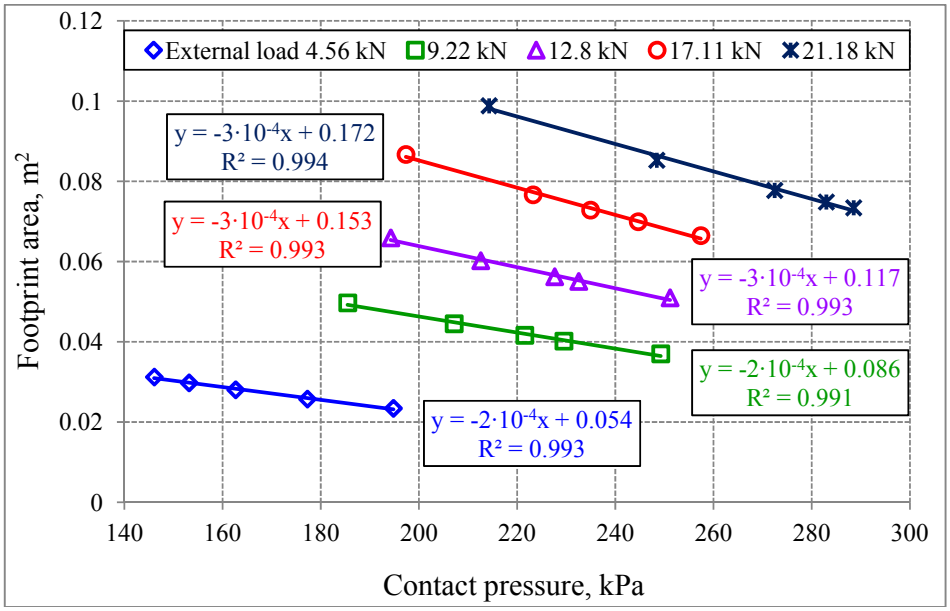

Fig. 5. Variation of footprint area depending on the contact pressure, for various external loads

It can be observed the distinguishing arrangement of the variation lines in a relatively wide range of values. If the variation of the footprint area depending on the contact pressure, for the external load of 4.56 kN, is disposed to the left of the diagram, at its bottom (which shows low values of the contact pressure and the footprint area), the range of values of the footprint area for an external load of 21.18 kN is disposed in the top right corner of the diagram, with a wide range of values of contact pressure and footprint area (which shows higher values of the contact pressure and the footprint area). However, if the ranges of contact pressure are overlapping for the five values of the external load, it can be seen that the

footprint area values (for the five series of values given by different values of the external load) are quite distinct, with only a short overlap in the high values of external load (i.e. 17.11 kN and 21.18 kN). It can also be noticed that the contact pressure values are between 145 and 195 kPa for an external load of 4.56 kN, corresponding to footprint area values between 0.023 and 0.032 m^2, these values widening for larger external loads. Thus, at 21.18 kN loading for contact pressures between 215 and 290 kPa, values of footprint area vary between 0.072 and 0.1 m^2, with lower values of the footprint area at higher values of contact pressure. Referring to this variation, it can be noted that all regression lines have slightly decreasing slope, and values of the slopes are still different from one external load to another (regression lines are not parallel). As an observation, extreme values of the range of variation of the footprint area with contact pressure, for five external loads, are disposed on two sigmoid curves, opening towards higher values of analyzed parameters.

The variation of the footprint area depending on the ($b \cdot d$) product (where b is the width of the footprint and d is the diameter of the tire) is plotted in Figure 6. The regression lines show a relatively good correlation with the experimental points, in four of the five cases ($R^2 \geq 0.806$).

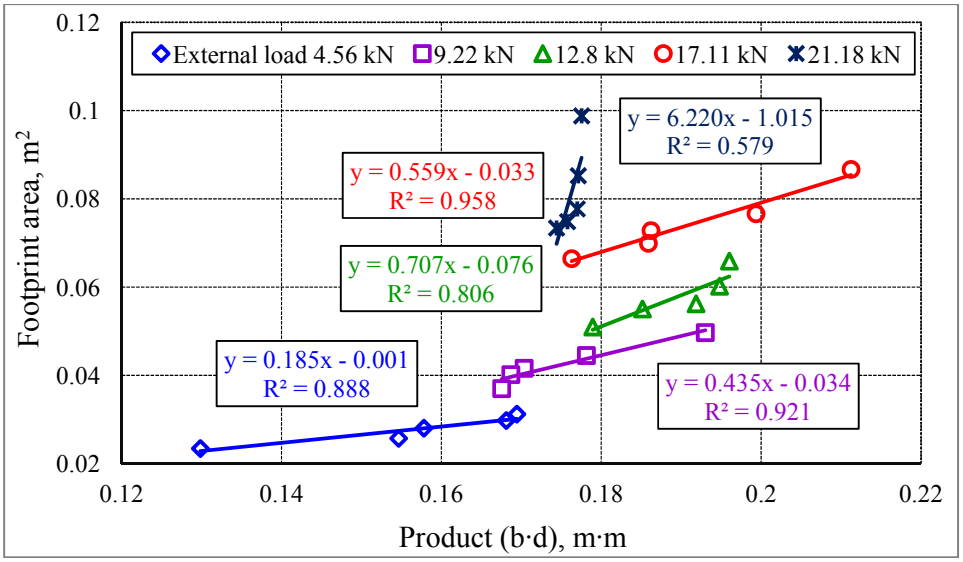

Fig. 6. Variation of footprint area depending on the (b·d) product, for various external loads

The diagram in Fig. 6 shows that the values of footprint area (for five external loads) depending on the ($b \cdot d$) product are very different and unequal, the most extended range of values is presented by the 17.11 kN load and the narrower by 21.18 kN load. However, regression lines are distinct, which shows that there

is a close correspondence between the three analyzed parameters ($b \cdot d$ product, footprint area and external load). It can be noticed that the ($b \cdot d$) product has lower values for lower external loads and increases with it to loads higher than 15 – 16 kN, then the values remain relatively constant, although footprint area increases for each value of the load. Also, the regression lines obtained for each series of experiments at different external loads, have an increasing slope with the increase of the ($b \cdot d$) product, and the slope of lines is even greater as the external load is also higher, like a fan opening, but with a significant shift to the right side of the diagram, where the values of the ($b \cdot d$) product are higher. The absolute values of footprint area range between 0.023 and 0.031 m^2, for values of the ($b \cdot d$) product between 0.13 and 0.17 m·m, for an external load of 4.56 kN. These values increase to between 0.051 and 0.066 m^2 for values of the ($b \cdot d$) product between 0.178 and 0.196 m·m, obtained for an external load of 12.8 kN. They also increase about 0.073 and 0.099 m^2 for values of the ($b \cdot d$) product between 0.174 and 0.178 m·m, for an external load of 21.18 kN. For an external load of 17.11 kN, the ($b \cdot d$) product values range between 0.176 and 0.211 m·m and their corresponding footprint areas were between 0.067 and 0.087 m^2 (more broadly than for other loads). For an external load of 9.22 kN, the obtained footprint area was between 0.036 and 0.049 m^2 for values of the ($b \cdot d$) product between 0.167 and 0.193 m·m.

Fig. 7 presents the variation of the footprint area depending on the (Q/p_i) ratio (external load / tire inflation pressure) for five values of the external load.

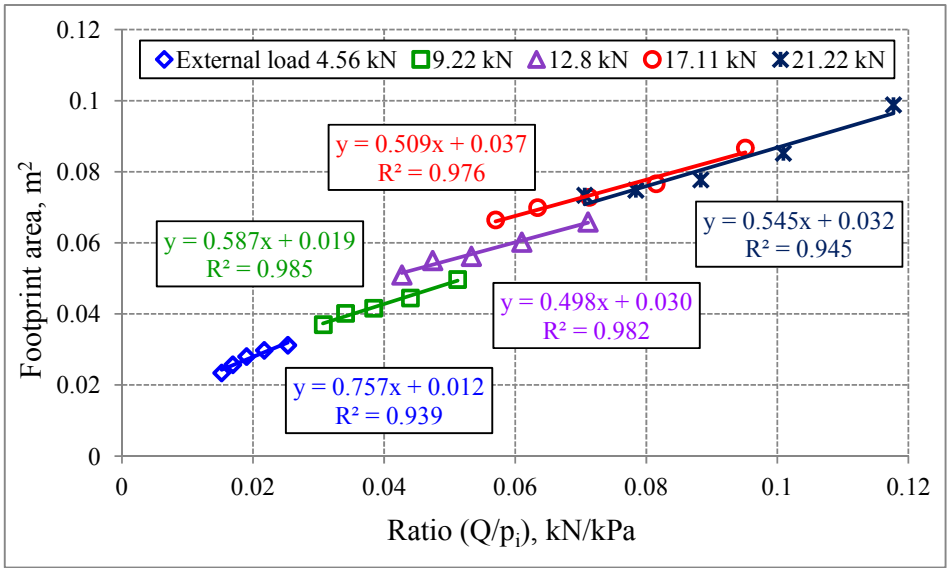

Fig. 7. Variation of footprint area depending on Q/p_i ratio, for various external loads

It was found that the values of the footprint area are distributed approximately linearly with the (Q/p_i) ratio, for each value of the external load,

and the regression lines are also about one in extension of the other, from the lowest to the highest load. The linear regression based on the experimental points for each of the five values of the external load, resulted in correlation coefficients $R^2 \geq 0.939$. Also, performing the regression analysis of all values from the five experimental sets, for footprint area depending on the (Q/p_i) ratio, a value of the correlation coefficient $R^2 = 0.985$ was obtained with the linear distribution law, which confirms the findings presented above.

5. Conclusions

The intensity of artificial compaction, induced by agricultural vehicles, depends on: soil properties (structure, texture, moisture content); size of external load; contact pressure (determined by tire size, tire inflation pressure and external load); number of passes on the soil.

In contact with a rigid surface, the tire of agricultural machinery deforms both longitudinally and transversely, and footprint size and shape are determined by the tire inflation pressure and by the size of external load (wheel load).

From the data presented in this paper it can be observed that the footprint area follows an approximately linearly distribution, proportional to the external load, regardless the tire inflation pressure. At tire inflation pressures between 180 and 300 kPa and external loads of 4.56 kN, footprint area is between 0.023 and 0.03 m^2, respectively between 0.0734 and 0.1 m^2 for external loads of 21.18 kN.

Also, experimental results have confirmed that by increasing tire inflation pressure, footprint area will decrease, however this decrease is a slow one. Values of contact pressure vary between 145 and 195 kPa for a wheel load of 4.56 kN, corresponding to footprint area values between 0.023 and 0.032 m^2, and these valuesincreased for greater external loads.

REFERENCES

[1] *K. Barik, E. L. Aksakal, K. R. Islam, S. Sari, I. Angin*, Spatial variability in soil compaction properties associated with field traffic operations. Catena, **vol. 120**, pp. 122-133, 2014.

[2] *Y. Bédard, S. Tessier, C. Laguë, Y. Chen, L. Chi*, Soil compaction by manure spreaders equipped with standard and oversized tires and multiple axles. Transactions of the ASAE, **vol 40(1)**, pp. 37-43, 1997.

[3] *S. Şt. Biriş*, Modelarea matematică a compactării solului agricol. Editura Printech, Bucureşti, 2010.

[4] *S. Şt. Biriş, N. Ungureanu, E. Maican, G. Paraschiv, Gh. Voicu, M. Manea*, FEM model for the study of interaction between the driving wheel and the rolling track for agricultural vehicles. 39th International Symposium "Actual Tasks on Agricultural Engineering", Croaţia, Opatija, pp. 95-105, 2011.

[5] *K.Y. Chan, A. Oates, A.D. Swan, R.C. Hayes, B.S. Dear, M.B. Peoples*, Agronomic consequences of tractor wheel compaction on a clay soil. Soil and Tillage Research, 2005.

[6] *S.O. Chung, K.A Sudduth, J.W. Hummel*, Design and validation of an on-the-go soil strength profile sensor. Transactions of the ASABE., **vol. 49(1)**, pp. 5-14, 2006.
[7] *K. Cui, P. Defossez, G. Richard*, A new approach for modeling vertical stress distribution at the soil/tyre interface to predict the compaction of cultivated soils by using the PLAXIS code. Soil & Tillage Research, **vol. 95**, pp. 277-287, 2007.
[8] *S. W. Duiker*, Effects of soil compaction. Publication code: UC188.
[9] *T. Ghezzehei, D. Or*, Rheological properties of wet soils and clays under steady and oscillatory stresses. Soil Sci. Soc. Am. J., **vol. 65**, pp. 624-637, 2001.
[10] *M. Gysi*, Soil compaction due to heavy agricultural wheel traffic. Swiss Federal Institute of Technology, Zurich, Switzerland, 2000.
[11] *M. Gysi, V. Maeder, P. Weisskopf*, Pressure distribution underneath tyres of agricultural vehicles. Transactions of the ASABE, **vol. 44 (6)**, pp. 1385-1389, 2001.
[12] *M. A. Hamza, W. K. Anderson*, Soil compaction in cropping systems. A review of the nature, causes and possible solutions. Soil & Tillage Research, **vol. 82**, pp. 121-145, 2005.
[13] *A. Hemmat, V. I. Adamchuck*, Sensor systems for measuring soil compaction: Review and analysis. Computers and Electronics in Agriculture, **vol. 63**, pp. 89-103, 2008.
[14] *J. W. Hummel, I. S. Ahmad, S. C. Newman, K. A. Sudduth, S. T. Drummond*, Simultaneous soil moisture and cone index measurement. Transactions of the ASAE, **vol. 47(3)**, pp. 607-618, 2004.
[15] *T. Keller, M. Lamandé*, Challenges in the development of analytical soil compaction models. Soil & Tillage Research, **vol. 111**, pp. 54-64, 2010.
[16] *T. Keller, M. Lamandé*, From soil stress to soil deformation: current state of the research. NJF Report. Soil compaction – effects on soil functions and strategies for prevention. **vol. 8**, no. 1. Seminar 448. Helsinki, Finland, 2012.
[17] *G. R. Mari, Ji. Changying*, Influence of agricultural machinery traffic on soil compaction patterns, root development, and plant growth, overview. American-Eurasian J. Agric. & Environ. Sci., **vol. 3 (1)**, pp. 49-62, 2008.
[18] *J. O. Ohu, E. Mamman, M. N. Dammo*, Effect of load application on some physical properties of Firgi Vertisol. pp: 278-290 (iworx5.webxtra.net).
[19] *P. Schjønning, M. Lamande, F. A. Tøgersen, J. Arvidsson, T. Keller*, Modelling effects of tyre inflation pressure on the stress distribution near the soil-tyre interface. Biosystems Engineering 99: 119-133, Elsevier, 2008.
[20] *G. J. Schwab, L. W. Murdock, L. G. Wells*, Assessing and preventing soil compaction. UK Cooperative Extension Service. University of Kentucky – College of Agriculture, 2004.
[21] *H. Schwanghart*, Measurement of contact area, contact pressure and compaction under tires in soft soil. Proc. 10th International Conference of the International Society for Terrain-Vehicle Systems, Kobe, Japan, pg. 193-204, 1990.
[22] *T. R. Way, T. Kishimoto, E. C. Burt, A. C. Bailey*, Tractor tire aspect ratio effects on soil stresses and rut depth. Transactions of the ASABE, **vol. 40 (4)**, pp. 871-881, 1997.
[23] *D. Wulfsohn*, Soil-tire contact area. Advances in Soil Dynamics. ASABE, vol. 3, pp. 59-84, 2009.